Versatile Double-Cross-Linking Approach to Transparent, Machinable, Supercompressible, Highly Bendable Aerogel Thermal Superinsulators

AUTHOR(S):

Zu, Guoqing; Kanamori, Kazuyoshi; Shimizu, Taiyo; Zhu, Yang; Maeno, Ayaka; Kaji, Hironori; Nakanishi, Kazuki; Shen, Jun

A Versatile Double-Cross-Linking Approach to Transparent, Machinable, Super-Compressible, Highly Bendable Aerogel and Xerogel Thermal Superinsulators

*Guoqing Zu, *[a,c] Kazuyoshi Kanamori, *[a] Taiyo Shimizu,[a] Yang Zhu,[a] Ayaka Maeno,[b] Hironori Kaji,[b] Kazuki Nakanishi,[a] Jun Shen[c]*

[a]Department of Chemistry, Graduate School of Science, Kyoto University, Kitashirakawa, Sakyo-ku, Kyoto 606-8502, Japan

[b]Institute for Chemical Research, Kyoto University, Gokasho, Uji, Kyoto 611-0011, Japan

[c]Shanghai Key Laboratory of Special Artificial Microstructure Materials and Technology, Pohl Institute of Solid State Physics, Tongji University, Shanghai 200092, P. R. China

*Corresponding authors：
Email: guoqingzu@yahoo.com (G. Zu)
kanamori@kuchem.kyoto-u.ac.jp (K. Kanamori)

ABSTRACT: A facile yet versatile approach to transparent, highly flexible, machinable, superinsulating organic-inorganic hybrid aerogels and xerogels is presented. This method involves radical polymerization of a single alkenylalkoxysilane to obtain polyalkenylalkoxysilane, and subsequent hydrolytic polycondensation to afford a homogeneous, doubly cross-linked nanostructure consisting of polysiloxanes and hydrocarbon polymer units. Here we demonstrate that novel aerogels based on polyvinylpolysilsesquioxane (PVPSQ), polyallylpolysilsesquioxane (PAPSQ), polyvinylpolymethylsiloxane (PVPMS), and polyallylpolymethylsiloxane (PAPMS) are facilely prepared *via* this approach from vinyltrimethoxysilane (VTMS, or vinyltriethoxysilane VTES), allyltrimethoxysilane (ATMS, or allyltriethoxysilane ATES), vinylmethyldimethoxysilane (VMDMS), and allylmethyldimethoxysilane (AMDMS), respectively. These aerogels combine low density, uniform nanopores, high transparency, super-compressibility, high bendability, excellent machinability, and thermal superinsulation (λ=14.5-16.4 mW m^{-1} K^{-1}). More importantly, transparent, superflexible, superinsulating aerogel-like xerogels are obtained with PVPMS and PAPMS *via* highly scalable ambient pressure drying without any solvent exchange and modifications for the first time. This work will open a new way to transparent, highly flexible porous materials promising in the practical applications of thermal superinsulators, adsorbents, sensors, *etc*.

KEYWORDS: organic-inorganic hybrid, aerogel, double-cross-linking, superflexibility, superinsulation

INTRODUCTION

Aerogels are highly porous, low-density materials that have a three-dimensional interconnected open pore structure consisting of ultrafine nanoparticles. They are typically prepared by a sol-gel process to obtain hydrogels or alcogels followed by a specific drying process to replace the liquid solvent with air without destroying their delicate nanostructure. Due to their unique porous structures, many kinds of aerogel possess high specific surface area (SSA) and low thermal conductivity, which make them attractive as thermal superinsulators, [1,2] adsorbents, [3,4] catalyst supports, [5] energy storage materials, [6-8] etc. Because of their homogeneous nanostructure, some aerogels, especially silica aerogels, are transparent in the visible light wavelengths, which makes them ideal materials as thermally superinsulating windows for efficient energy savings in houses and buildings. [9,10] Aerogels are, however, usually mechanically weak (friable) resulting from their thin skeletons and their practical applications have been limited. Hybridization of aerogels with organic compounds is widely studied to improve their mechanical properties. [11-13] Unfortunately, most traditional organic-inorganic hybridization strategies resulted in a significant decrease in porosity, SSA and transparency and a significant increase in density and thermal conductivity.

A convenient organic-inorganic hybridization strategy to enhance their mechanical properties while maintaining their unique properties is to employ a trifunctional organotrialkoxysilane to obtain polyorganosilsesquioxane ($RSiO_{3/2}$) aerogels. Transparent polymethylsilsesquioxane (PMSQ), [14,15] polyethylsilsesquioxane (PESQ), and polyvinylsilsesquioxane (PVSQ) aerogels[16] were first obtained *via* this method from methyltrimethoxysilane (MTMS), ethyltrimethoxysilane (ETMS), and vinyltrimethoxysilane (VTMS), respectively. These aerogels are exceptionally strong and elastic against compression due to the lower crosslinking

density, low concentration of remaining silanol and abundant organic groups in the network. The compression flexibility enables ambient pressure drying (APD) of these gels to obtain aerogel-like xerogels that have almost the same properties and monolithicity as those of the corresponding aerogels obtained *via* high-pressure supercritical drying (SCD). Bending flexibility of these aerogels is, however, still limited and desired to be improved for better productivity, handling and extended applications. Another way to improve the mechanical properties is to use an organo-bridged alkoxysilane as a single precursor to prepare organo-bridged polysiloxane aerogels. [17,18] Benefiting from the organic bridge and its homogenous distribution in the network, some of them show bendability. [19-21] Nonetheless, their limited bendability still could not meet the need of practical applications.

Several biomass-based aerogels such as transparent nanocellulose and chitosan aerogels exhibit improved compressibility and bendability compared to those of traditional aerogels because of their robust skeletal structures consisting of interconnected flexible nanofibers. [22-24] Unlike the polysiloxane-based organic-inorganic hybrid aerogels, however, they do not show elastic recovery in response to compression and bending. It is reported that polymer-based aerogels such as supramolecular aerogel, [25] poly(vinyl alcohol)-based aerogel, [3] thermoelectric polymer aerogel[26] and resorcinol-formaldehyde aerogel[27] exhibit high mechanical strength or elasticity against compression. Nonetheless, almost all of them are mainly composed of macropores and are opaque in visible light region.

It is noteworthy that several reported wet gels or dense gel films show high mechanical strength. Polymer hydrogels with a double network structure containing discrete soft and rigid polymer networks were obtained by radical polymerization. [28-30] Although these two networks are interpenetrated and have no chemical cross-linking between them, a nonlinear effect of the

binary structure leads to high mechanical strength and flexibility of the materials. In addition, transparent and flexible hybrid dense gel films containing siloxane backbone linkages and polyethylene were obtained from VTMS *via* a combination of radical polymerization and hydrolytic polycondensation. [31,32] Inspired from these works, we have recently developed a facile yet general double-cross-linking approach for the preparation of transparent, highly flexible, superinsulating organic-inorganic hybrid aerogels and xerogels from a single alkenylalkoxysilane, vinylmethyldimethoxysilane (VMDMS). [33]

This double-cross-linking approach involves the radical polymerization of VMDMS in the presence of an initiator such as di-*tert*-butyl peroxide (DTBP) to obtain linear polyvinylmethyldimethoxysilane (PVMDMS) with controllable conversion and degree of polymerization, and subsequent hydrolytic polycondensation in the presence of a strong base catalyst, affording a doubly cross-linked, organic-inorganic hybrid polyvinylpolymethylsiloxane (PVPMS) network. This network consists of polysiloxanes and hydrocarbon chains that are chemically cross-linked with each other, which is different from the reported double network structure of hydrogels. We demonstrate here that novel polyvinylpolysilsesquioxane (PVPSQ), polyallylpolysilsesquioxane (PAPSQ), and polyallylpolymethylsiloxane (PAPMS) aerogels are facilely prepared *via* this approach from VTMS (or vinyltriethoxysilane VTES), allyltrimethoxysilane (ATMS, or allyltriethoxysilane ATES), and allylmethyldimethoxysilane (AMDMS), respectively, in addition to PVPMS. Benefiting from their unique doubly cross-linked structure, the optimized PVPSQ, PAPSQ, PVPMS, and PAPMS aerogels combine low density, high surface area, high transparency, high strength and flexibility against compression and bending, and superinsulating performances. It is noteworthy that, in the cases of PVPMS and PAPMS systems, transparent and superflexible

PVPMS and PAPMS aerogel-like xerogels have been successfully obtained *via* APD without any post-gelation modifications, showing a high potential for reducing the production cost and improved scalability. These superior properties combined with the facile approach allow these aerogels and xerogels to be promising in practical applications such as transparent thermal superinsulators, catalyst supports and sensors.

EXPERIMENTAL SECTION

Materials. Vinyltrimethoxysilane (VTMS), vinylmethyldimethoxysilane (VMDMS), and tetramethylammonium hydroxide (TMAOH) (25 wt % in water) were purchased from Sigma-Aldrich, Co. (USA). Allyltrimethoxysilane (ATMS), vinyltriethoxysilane (VTES), and di-*tert*-butyl peroxide (DTBP) were obtained from Tokyo Chemical Industry Co., Ltd. (Japan). Allylmethyldimethoxysilane (AMDMS) was obtained from Gelest, INC. (USA). Allyltriethoxysilane (ATES) was obtained from Shin-Etsu Chemical Co., Ltd. (Japan). Distilled water was obtained from Hayashi Pure Chemical Ind., Ltd. (Japan). Benzyl alcohol (BzOH), 2-propanol (IPA) and *n*-hexane were purchased from Kishida Chemical Co., Ltd. (Japan). All the chemical reagents were used as received.

Sample preparation. An appropriate amount of the precursor (VTMS, VTES, ATMS, ATES, VMDMS, or AMDMS) and initiator (DTBP, 1, 5, 10, or 20 mol%) were mixed and placed in a hydrothermal reactor. The reactor was sealed after flushing with Ar and then heated to 120 °C for 48 h. After cooling naturally to room temperature, a transparent and viscous liquid was obtained. These viscous liquids from precursors VTMS, VTES, ATMS, ATES, VMDMS, and AMDMS mainly contain linear polymers polyvinyltrimethoxysilane (PVTMS), polyvinyltriethoxysilane (PVTES), polyallyltrimethoxysilane (PATMS),

polyallyltriethoxysilane (PATES), polyvinylmethyldimethoxysilane (PVMDMS), and polyallylmethyldimethoxysilane (PAMDMS), respectively. BzOH, H_2O and TMAOH with a specific molar ratio were added into the above liquid in the listed order with stirring for 5 min. The sol was then transferred into a polypropylene container, which was then sealed and placed in a forced convection oven at 80 or 100 °C, where the gel formed within 1 h and was aged at this temperature for 4 d. The gels of PVPMS1, PVPMS2, and PVPMS3 were aged at 80 °C, while other gels including PVPMS1-X1 were aged at 100 °C. The obtained gel was washed with IPA at 60 °C three times (each 8 h) to remove the residual H_2O, BzOH, and other chemicals.

In the case of SCD, the gel was dried from supercritical carbon dioxide at 80 °C, 13.5 MPa to afford PVPSQ, PAPSQ, PVPMS, and PAPMS aerogels. In the case of APD from alcohol (IPA), the gel was slowly dried *via* evaporation at room temperature for 2-5 d and at 80 °C for 4 h to obtain a xerogel. In the case of APD from *n*-hexane, the gel was washed with *n*-hexane at 50 °C three times (each 8 h), after which it was slowly dried *via* evaporation at room temperature for 2 d and at 80 °C for 4 h to obtain a xerogel.

In order to obtain PVPMS xerogels (PVPMS1-X2, PVPMS2-X2) *via* ultralow-cost APD without any solvent exchange and modifications, the wet gels were prepared by using IPA as the solvent instead of BzOH. After vigorous aging at 120 °C in a sealed container for 4 d, the wet gel was directly dried *via* evaporation at room temperature for 2-5 d and at 80 °C for 4 h without any solvent exchange and post-modifications.

Characterizations. The weight-average molecular weight (M_w), degree of polymerization and polydispersity (M_w/M_n) of PVTMS, PATMS, PVMDMS, and PAMDMS were determined by a gel permeation chromatography (GPC) system (GPC104, Shodex, Japan). A LF604

column and chloroform solvent were used during the GPC measurement. The conversion of PVTMS, PATMS, PVMDMS, and PAMDMS was calculated from the ^{1}H nuclear magnetic resonance (NMR) spectra, which was measured in $CDCl_3$ using an NMR spectrometer (Avance III 800US Plus, Bruker Corp., Germany) operating at 800 MHz.

The bulk density of aerogels and xerogels was calculated by equation $\rho = m/V$, where m is the mass and V is the volume of the gel. The Fourier transform infrared (FTIR) spectra was obtained with an FTIR spectroscope (IRAffinity-1, Shimadzu Corp., Japan). The morphology of aerogels and xerogels was observed by a field emission scanning electron microscope (FESEM, JSM-6700F, JEOL, Japan). The visible-light transmittance (at 550 nm) was obtained from the UV-vis-NIR spectra measured with a UV-vis-NIR spectrophotometer (V-670, JASCO, Japan) equipped with an integrating sphere. Contact angles of water were determined using a Drop Master (DM-561Hi, Kyowa Interface Science Co., Ltd., Japan). The solid-state structure was investigated by the ^{29}Si cross-polarization magic angle spinning (CP/MAS) NMR spectra using an NMR spectrometer (Avance III 800US Plus, Bruker Corp., Germany). It was operated at a static magnetic field of 18.8 T with the probe of 4 mm. For all the samples, the MAS frequency was 12 kHz, the contact time for CP process was 7 ms, the recycle delay was 4 s, and the number of scan was 4069. Hexamethylcyclotrisiloxane was used as an external reference material at -9.66 ppm.

The SSA and pore size distribution were obtained from the N_2 adsorption/desorption isotherm measured with a N_2 adsorption analyzer (BELSORP-mini, BEL Japan, Inc., Japan). The sample was degassed at 100 °C under vacuum for 6 h before the measurement. The Brunauer-Emmett-Teller (BET) method was used to calculate the SSA from the adsorption branch of the isotherm. The Barrett-Joyner-Halenda (BJH) method was used to determine the

pore size distribution from the adsorption branch of the isotherm.

The mechanical properties (compression and bending) of aerogels and xerogels were studied by the uniaxial compression-decompression tests and three-point bending tests carried out with a material tester (EZGraph, Shimadzu Corp., Japan). The crosshead speed during the compression and bending tests was kept at 0.5 mm min^{-1}. A cylindrical aerogel with diameter × height of (8-15) × (4-10) mm was used for the uniaxial compression-decompression tests. A sheet-shaped aerogel with width × length × thickness of 10 × (50−60) × 1 mm was used for the three-point bending tests. The fixture span during the three-point bending tests was fixed at 25 mm.

The thermal stability of the samples was studied by thermogravimetric-differential thermal analysis (TG-DTA) with a Thermo plus EVO (TG 8120, Rigaku Corp., Japan). The samples were heated with a rate of 5 °C min^{-1} in air. The thermal conductivity at room temperature and ambient pressure was measured using a heat flow meter (HFM 436 Lambda, NETZSCH, Germany). An aerogel with typical width × length × height of 100 × 100 × 10 mm was used.

RESULTS AND DISCUSSION

The synthesis procedures of transparent PVPSQ, PAPSQ, PVPMS, and PAPMS aerogels and xerogels *via* the double-cross-linking method are presented schematically in Figure 1. The character “PVPSQ”, “PAPSQ”, “PVPMS”, and “PAPMS” in the sample names indicates the PVPSQ, PAPSQ, PVPMS, and PAPMS aerogel, respectively. The numbers 1, 2, or 3 are relevant to the different molar ratio of benzyl alcohol (BzOH) to the precursor (VTMS, ATMS, VMDMS, or AMDMS). The percent values, “5%” and “10%”, indicate the concentration of the radical initiator DTBP. The character “X1” indicates the xerogels by APD from alcohol or

n-hexane without any modifications. The "X2" indicates the xerogels by APD *without any solvent exchange and modifications*. Since the costly and time-consuming solvent exchange and surface modification processes have been two of the highest barriers in a massive production of aerogels, this APD process without any solvent exchange and modifications is considerably advantageous for realistic industrialization. For these four kinds of aerogels and xerogels, temperature and time during radical polymerization are fixed at 120 °C and 48 h, respectively. The DTBP concentration was varied in the range of 1 to 20 mol%. The results on the radical polymerization of VTMS, ATMS, VMDMS, and AMDMS are shown in Table S1. Under the DTBP concentration of 20 mol%, the molecular weight of the resulting polyvinyltrimethoxysilane (PVTMS), polyallyltrimethoxysilane (PATMS), and polyallylmethyldimethoxysilane (PAMDMS) is 22961, 3510, and 3399, respectively. The PVTMS exhibits a higher degree of polymerization (155) compared to those of PATMS (22) and PAMDMS (23), while the M_w/M_n is higher (6.35). Meanwhile, the PVTMS, PATMS, and PAMDMS exhibit high conversion of >99%, 97%, and 91%, respectively. The resulting PVMDMS also shows a high degree of polymerization of 41-68 and high conversion of 97-99% under the DTBP concentration of 1-5 mol%.

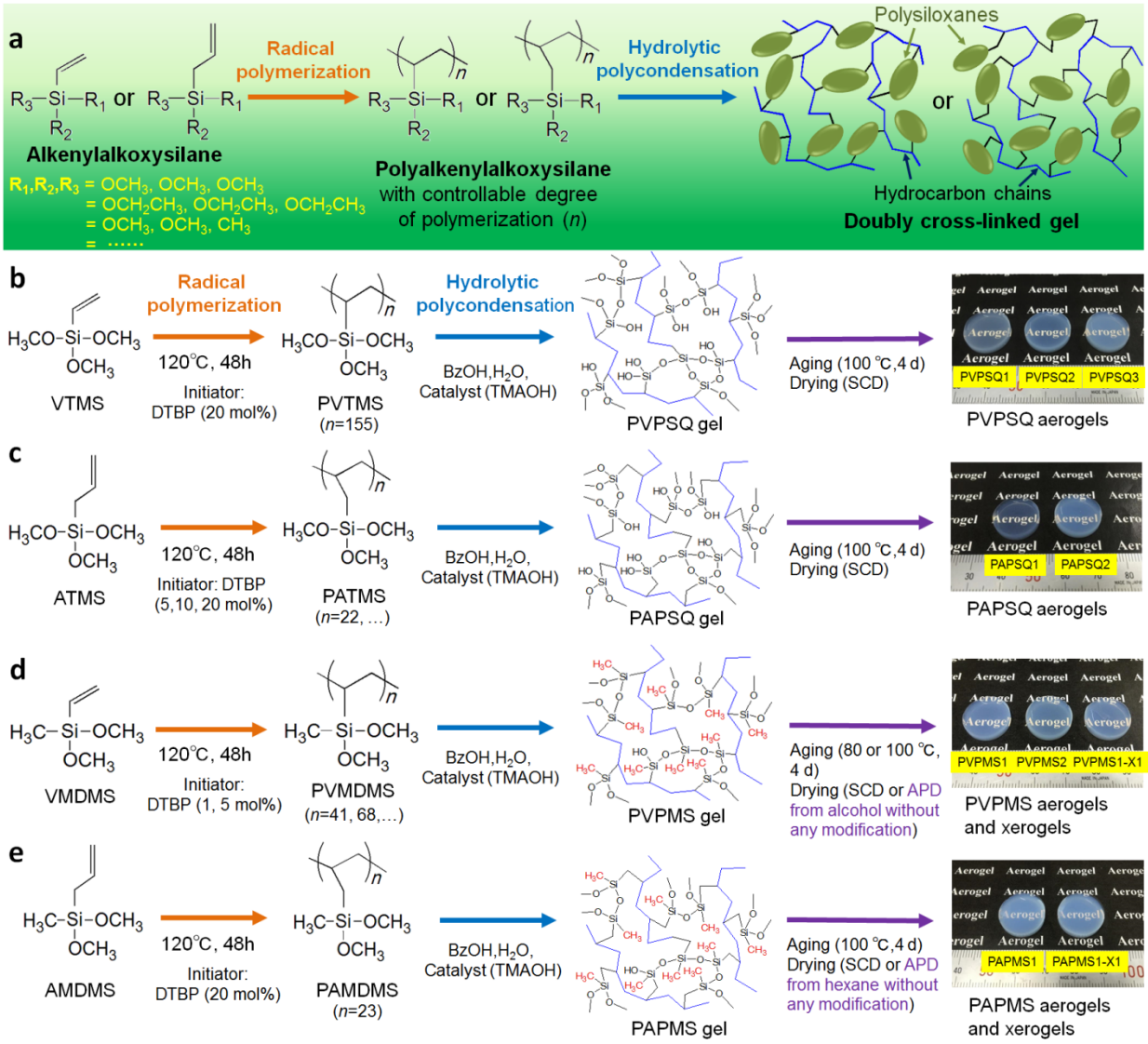

Figure 1. The double-cross-linking method and resultant aerogels/xerogels. (a) Schematic of synthesis of organic-inorganic hybrid aerogels *via* the versatile double-cross-linking method. Each synthesis scheme and resultant aerogels/xerogels of (b) PVPSQ, (c) PAPSQ, (d) PVPMS, and (e) PAPMS from precursors VTMS, ATMS, VMDMS, and AMDMS, respectively.

Direct hydrolysis and polycondensation of trifunctional precursors VTMS and ATMS tend to induce macroscopic phase separation between the polar solvent and hydrophobic condensates with vinyl or allyl groups, unless the reaction system is carefully designed.[16] The macroscopic

phase separation usually results in precipitations or heterogeneous gels with low or no transparency and porosity. In the case of VMDMS and AMDMS, direct hydrolysis and polycondensation do not afford a three-dimensional network structure since it contains only two hydrolyzable groups. In our approach, the radical polymerization of VTMS, ATMS, VMDMS, and AMDMS affords linear PVTMS, PATMS, PVMDMS, and PAMDMS, respectively, with a large number of hydrolyzable alkoxy groups in each polymer molecule, which lowers the tendency of macroscopic phase separation and contributes to homogenous gelation. Besides, a strong base (tetramethylammonium hydroxide, TMAOH) is used as the hydrolysis and polycondensation catalyst to promote more accelerated gelation prior to macroscopic phase separation. This is supposed to afford a doubly cross-linked porous structure with increased homogeneity.

The doubly cross-linked structure with the co-presence of polysiloxanes and aliphatic hydrocarbon chains is confirmed by solid-state ^{29}Si NMR (Figure 2a,b) and FTIR spectra (Figure 2c). As shown in Figure 2a,b and the multiple peak fitting of the NMR spectra (Figure S1), the intense peaks located at around -64, -66, -19, and -22 ppm correspond to T^3 $(CH_2CH(SiO_{3/2}))_n$ and T^2 species[16] in the PVPSQ aerogels, T^3 $(CH_2CH(CH_2SiO_{3/2}))_n$ and T^2 species[34] in the PAPSQ aerogels, D^2 $(CH_2CH(Si(CH_3)O_{2/2}))_n$ and D^1 species in the PVPMS aerogels, and D^2 $(CH_2CH(CH_2Si(CH_3)O_{2/2}))_n$ and D^1 species in the PAPMS aerogels, respectively.[19] For PAPMS aerogels, the small peak at around -36 ppm is attributed to a small amount of silicon with unpolymerized allyl groups in CH_2=$CHCH_2Si(CH_3)O_{2/2}$. For PVPMS and PAPMS aerogels, the small peak recognized at around -68 ppm can be attributed to T^3 ($RSiO_{3/2}$, R may be methyl) species that are probably derived from the reaction between allylsilane or vinylsilane and silanol to form a siloxane bond and T silicon.[35,36] The similar

reaction also occurs in PVPSQ and PAPSQ systems to give a certain amount of Q silicon species (around -100 ppm), but it is negligible in these samples.

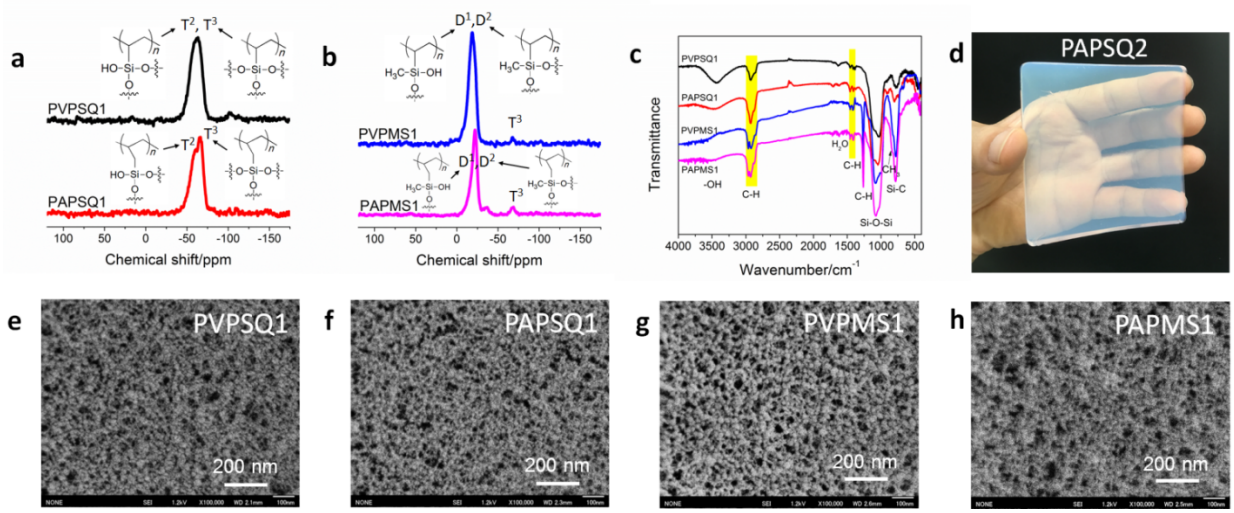

Figure 2. Apparence and structures of typical aerogels. (a,b) Solid-state ^{29}Si CP/MAS NMR spectra, (c) FTIR spectra, (d) photograph, and (e-h) FESEM images of typical PVPSQ, PAPSQ, PVPMS, and PAPMS aerogels.

Besides, as presented in Figure 2c, the bands located at 1406 cm^{-1} and 1456 cm^{-1} are ascribed to the symmetric deformation and bending of C-H bonds, respectively, while the bands located at 2865 cm^{-1}, 2923 cm^{-1}, and 2964 cm^{-1} are attributed to the stretching of C-H bonds.[37-39] These bands mainly result from the aliphatic hydrocarbon chains of PVPSQ and PAPSQ aerogels, and the hydrocarbon chains plus methyl groups of PVPMS and PAPMS aerogels. It is noteworthy that, unlike PVPSQ and PAPSQ aerogels, the PVPMS and PAPMS aerogels show intense absorption bands at 780 cm^{-1}, ~818 cm^{-1} and 1260 cm^{-1} corresponding to the asymmetric stretching of Si-C bonds, rocking of CH_3 and asymmetric deformation of C-H bonds,[37] respectively, indicating the methyl-rich polymethylsiloxane structure of PVPMS and

PAPMS aerogels. Meanwhile, the weaker broad bands located between 3000 cm^{-1} and 3600 cm^{-1} corresponding to the stretching of –OH, indicating the lower concentration of –OH groups in PVPMS and PAPMS aerogels compared to those in PVPSQ and PAPSQ aerogels. Accordingly, the PVPSQ and PAPSQ aerogels are more hydrophilic while the PVPMS and PAPMS aerogels are highly hydrophobic (Figure S2). There is no absorption band corresponding to allyl groups in the FTIR spectra even if it is identified by NMR, indicating that the amount of residual allyl groups in PAPMS aerogels is sufficiently small. In addition, these four kinds of aerogels are thermally stable up to approximately 210 °C, above which thermal oxidation of the hydrocarbon chains and $–CH_3$ groups occurs (Figure S3).

The porous structure of these samples has been investigated by FESEM and N_2 adsorption/desorption measurements. As shown in FESEM images (Figures 2e-h and S4), the obtained PVPSQ, PAPSQ, PVPMS, and PAPMS aerogels exhibit a homogeneous three-dimensional porous network structure consisting of aggregated nanoparticles smaller than 50 nm. Meanwhile, all the samples show narrow pore size distributions (the inset of Figure S5) with pore sizes mainly in the range of 10-70 nm. Since the radical polymers PVTMS and PATMS have a larger number of hydrolyzable alkoxy groups that form less hydrophobic networks, the tendency of macroscopic phase separation is lower than that of the networks from PVMDMS and PAMDMS. Consequently, the PVPSQ and PAPSQ aerogels show a more homogeneous porous structure with smaller particle and pore sizes compared to those of PVPMS and PAPMS aerogels.

These four kinds of aerogels exhibit high SSAs; the SSAs of PVPSQ and PAPSQ aerogels (965-1059 $m^2\ g^{-1}$) are higher than those of PVPMS and PAPMS aerogels (768-950 $m^2\ g^{-1}$). It is also observed from the FESEM images (Figures 2e-h and S4) and pore size distributions (the

inset of Figure S5) that the pore and particle sizes of all the samples increase with the decrease of bulk density in the range of 0.13-0.26 g cm^{-3}. This is because the tendency for homogeneous gelation becomes lower when the precursor concentration is decreased. The DTBP concentration in the radical polymerization also affects the microstructure of the resulting aerogels (Table S2 and Figure S6).

Table 1. Starting compositions and typical properties of doubly cross-linked PVPSQ, PAPSQ, PVPMS, and PAPMS aerogels/xerogels [a].

sample		DTBP /mol%	t_p [b] /h	BzOH/Si /mol mol^{-1}	H_2O/Si /mol mol^{-1}	TMAOH/Si /mol mol^{-1}	ρ [c] /g cm^{-3}	S_{BET} [d] /m^2 g^{-1}	d [e] /nm	T [f] /%	λ [g] /mW m^{-1} K^{-1}
PVPSQ aerogel	PVPSQ1	20	48	4.4	3	0.015	0.22	1029	28	90	
	PVPSQ2	20	48	5.9	3	0.015	0.17	965	44	88	15.0
	PVPSQ3	20	48	7.4	3	0.030	0.13	989	58	83	
PAPSQ aerogel	PAPSQ1	20	48	4.9	3	0.033	0.22	1059	24	94	
	PAPSQ2	20	48	6.5	3	0.067	0.18	1021	37	88	15.3
PVPMS aerogel/ xerogel	PVPMS1	1	48	4.3	2	0.030	0.22	950	32	82	15.3
	PVPMS2	1	48	5.0	2	0.045	0.19	919	44	76	15.2
	PVPMS3	5	48	7.2	2	0.125	0.13	927	66	63	14.5
	PVPMS1-X1	1	48	4.3	2	0.030	0.21	903	44	80	15.4
	PVPMS1-X2	1	48	5.9(IPA/Si)	2	0.030	0.23	770	37	78	
	PVPMS2-X2	1	48	6.8(IPA/Si)	2	0.045	0.19	716	58	70	
PAPMS aerogel/ xerogel	PAPMS1	20	48	4.1	2	0.050	0.26	778	37	70	
	PAPMS1-X1	20	48	4.1	2	0.050	0.26	766	37	71	
	PAPMS2	20	48	4.9	2	0.058	0.23	768	50	61	16.4

[a] For a typical sample PVPMS1, the volumes of VMDMS, BzOH, H_2O, and 2.8M TMAOH are 1, 3, 0.188, and 0.071 mL, respectively. [b] Reaction time of radical polymerization. [c] Bulk density. [d] SSA obtained from nitrogen adsorption measurement. [e] Mean pore diameter. [f] Visible-light transmittance at 550 nm for 2 mm thick aerogel. [g] Thermal conductivity at room temperature and ambient pressure.

Due to the homogeneous structure and pore and particle sizes mainly smaller than 70 nm, all these four kinds of aerogels are transparent in visible light region as shown in Figures 1 and 2d.

The 2 mm thick PVPSQ and PAPSQ aerogels exhibit a high visible-light transmittance of 83-94% (Table 1). The transmittance of 2 mm thick PVPMS aerogels with bulk density of 0.16-0.22 g cm^{-3} is 76-82%. Although the transmittance of PAPMS aerogels is lower due to the relatively larger pore and particle sizes, the value of which is still above 60% for a 2 mm thick PAPMS aerogel. For all the samples, the transparency decreases moderately with the decrease of density due to the increase of pore and particle sizes. Due to the co-presence of methyl-rich, intrinsically hydrophobic polymethylsiloxanes and hydrocarbon chains, the optimized PVPMS and PAPMS wet gels can be successfully dried by APD from *n*-hexane or 2-propanol (IPA) without any modifications to afford crack-free transparent PVPMS and PAPMS aerogel-like xerogel monoliths (Figure 1d,e). During the process of APD from *n*-hexane, the PAPMS1-X1 wet gel undergoes a large temporal shrinkage (around 23% in linear) resulting from the capillary force exerted on the entire gel skeletons. However, the gel finally springs back to nearly their original size after they are totally dried. The PVPMS1-X1 wet gel during the process of APD from IPA exhibits the similar behavior. This behavior is attributed to their unique doubly cross-linked elastic structure with abundant aliphatic hydrocarbon chains and methyl groups and a small amount of –OH groups.

The resulting PVPMS and PAPMS xerogels exhibit comparable molecular- and nano-scaled structures to those of the corresponding PVPMS and PAPMS aerogels, respectively. Transparency (80% and 71% transmittance, Table 1), morphology (Figure S4d,e), particle size (mainly 10-50 nm), pore size (mainly 10-60 and 10-45 nm) and SSA (903 and 766 $m^2 g^{-1}$) of PVPMS1-X1 and PAPMS1-X1 are similar to those of the aerogels PVPMS1 and PAPMS1, respectively. Since PVPMS and PAPMS aerogel-like xerogels are obtained by APD without any modifications that consume solvent, surface modifiers and processing time, they show a high

potential for reducing the production cost and high scalability without a need for high-pressure autoclaves. In addition, alcohols as the drying solvent are advantageous to reduce the solvent-exchange steps since they are miscible with the original aqueous pore liquid while hydrocarbons like *n*-hexane are not.

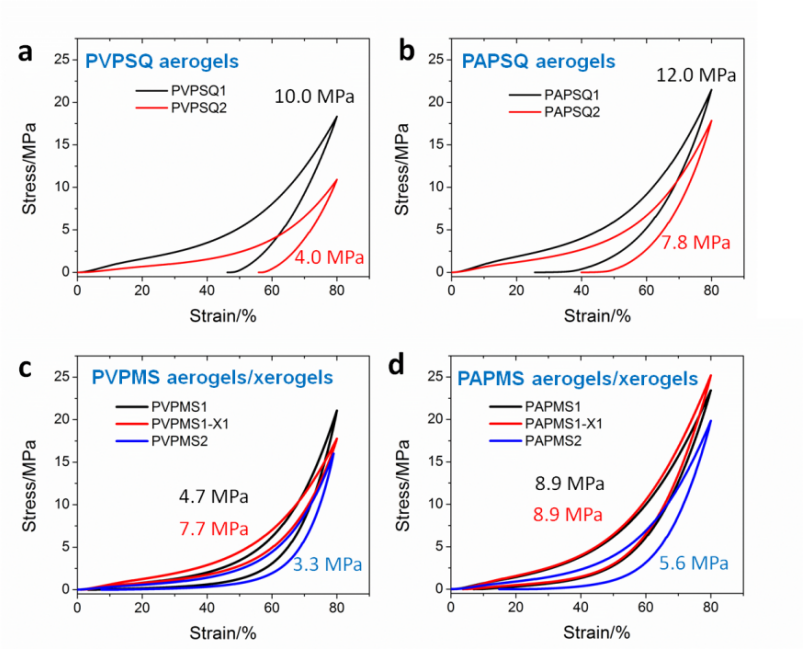

Figure 3. Stress-strain curves of uniaxial compression-decompression tests on typical (a) PVPSQ, (b) PAPSQ, (c) PVPMS, and (d) PAPMS aerogels/xerogels. The values in the figure are the obtained Young's moduli.

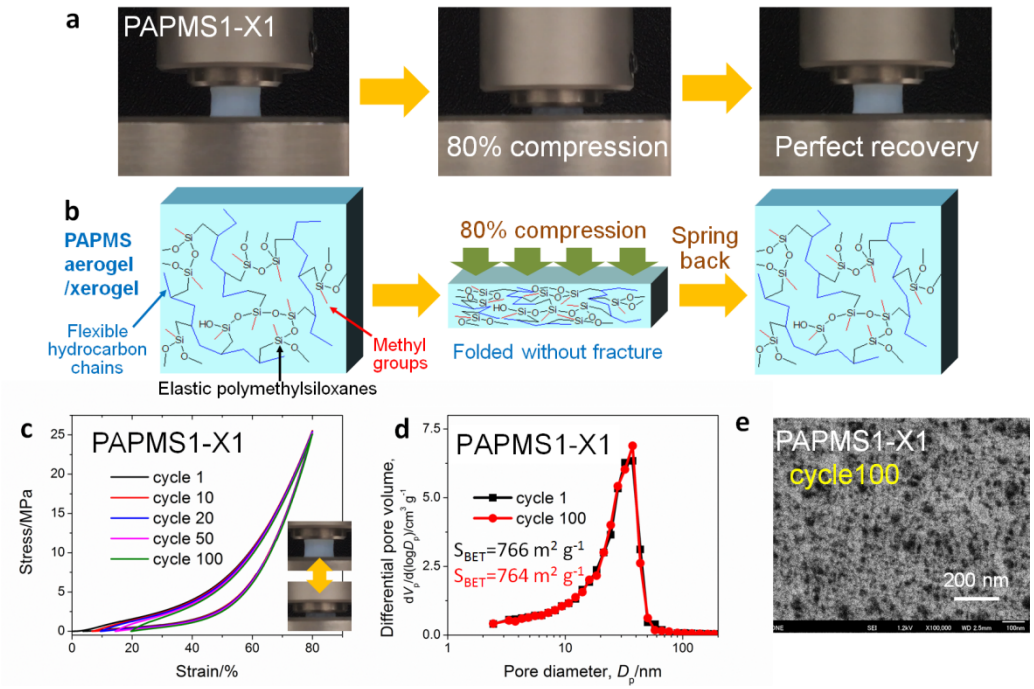

Figure 4. (a) Photographs of a uniaxial compression-decompression test on PAPMS xerogel PAPMS1-X1. (b) Schematic of molecular-scaled structure variations of PAPMS aerogel/xerogel during compression-decompression, mainly occurring in the neck part of the colloidal skeletons. (c) Stress-strain curves of 100 cycles of uniaxial compression-decompression on PAPMS1-X1. (d) BJH pore size distribution and (e) FESEM image of PAPMS1-X after the compression-decompression with 80% strain for 100 cycles, exhibiting no visible changes.

Benefiting from their unique doubly cross-linked structure with the co-presence of polysiloxanes and hydrocarbon chains, the PVPSQ, PAPSQ, PVPMS, and PAPMS aerogels and xerogels exhibit outstanding mechanical properties. As shown in Figure 3, all these four kinds of aerogels show high compression flexibility. In the cases of PVPSQ and PAPSQ aerogels, they are compressed with 80% strain without fracture and partially recover their original sizes after the force is removed. The PVPSQ1 and PAPSQ1 gels spring back to 54% and 75%, respectively, immediately after the force is removed (Figure 3a,b) and continue to spring back

to around 60% and 82%, respectively, after 4 h at room temperature. In the cases of PVPMS and PAPMS aerogels and xerogels, they are compressed with 80% strain without fracture and perfectly recover their original sizes after the force is removed (Figures 3 and 4a,b), showing superelasticity against compression. Apparently, the elasticity against compression increases in the following order: PVPSQ aerogels < PAPSQ aerogels < PAPMS aerogels ≈ PVPMS aerogels. Movie S1 clearly demonstrates the super-compressibility and superelasticity of PAPMS1-X1. It should be noted that PAPMS1-X1 springs back to around 80% of its original size immediately after the compression-decompression with 80% strain for 100 cycles (Figure 4c) and continues to spring back to around 89% after 10 min at room temperature and finally perfectly recovers its original size after heat treatment at 120 °C for 1 h. The spring-back of the folded flexible skeletons is due to the relaxation of polysiloxanes and hydrocarbon chains and repulsion of methyl groups, which are accelerated at higher temperatures. Its morphology, SSA and pore size distribution remain virtually unchanged after the compression-decompression for 100 cycles (Figure 4d,e). In addition, all these aerogels exhibit high Young's moduli of 10.0, 12.0, 4.7, and 8.9 MPa for PVPSQ1, PAPSQ1, PVPMS1, and PAPMS1, respectively.

Moreover, as presented in Figures 5 and S7, the PVPSQ, PAPSQ, PVPMS, and PAPMS aerogels exhibit high bending flexibility. They undergo a large diametral deformation of around 7-30 mm in the three-point bending tests with a fixture span of 25 mm and recover nearly their original shapes after the forced is removed. By comparing the photographs of hand bending tests and stress-strain curves of these four kinds of aerogels, the bending flexibility of PAPSQ aerogels is higher than that of PVPSQ aerogels, and the PVPMS and PAPMS aerogels exhibit even higher bending flexibility. The movies of hand bending tests (Movies S2 and S3) clearly show the superflexibility of PVPMS and PAPMS aerogels. It is noteworthy that the PAPMS

xerogel PAPMS1-X1 possesses comparable flexibility to that of the corresponding aerogel (Figure S8). Moreover, these four kinds of aerogels show excellent machinability. The monolithic samples with a desired shape can be obtained simply by cutting with a knife without fracture (Figures 6a,b and S9), which has never been reported in other transparent aerogel materials.

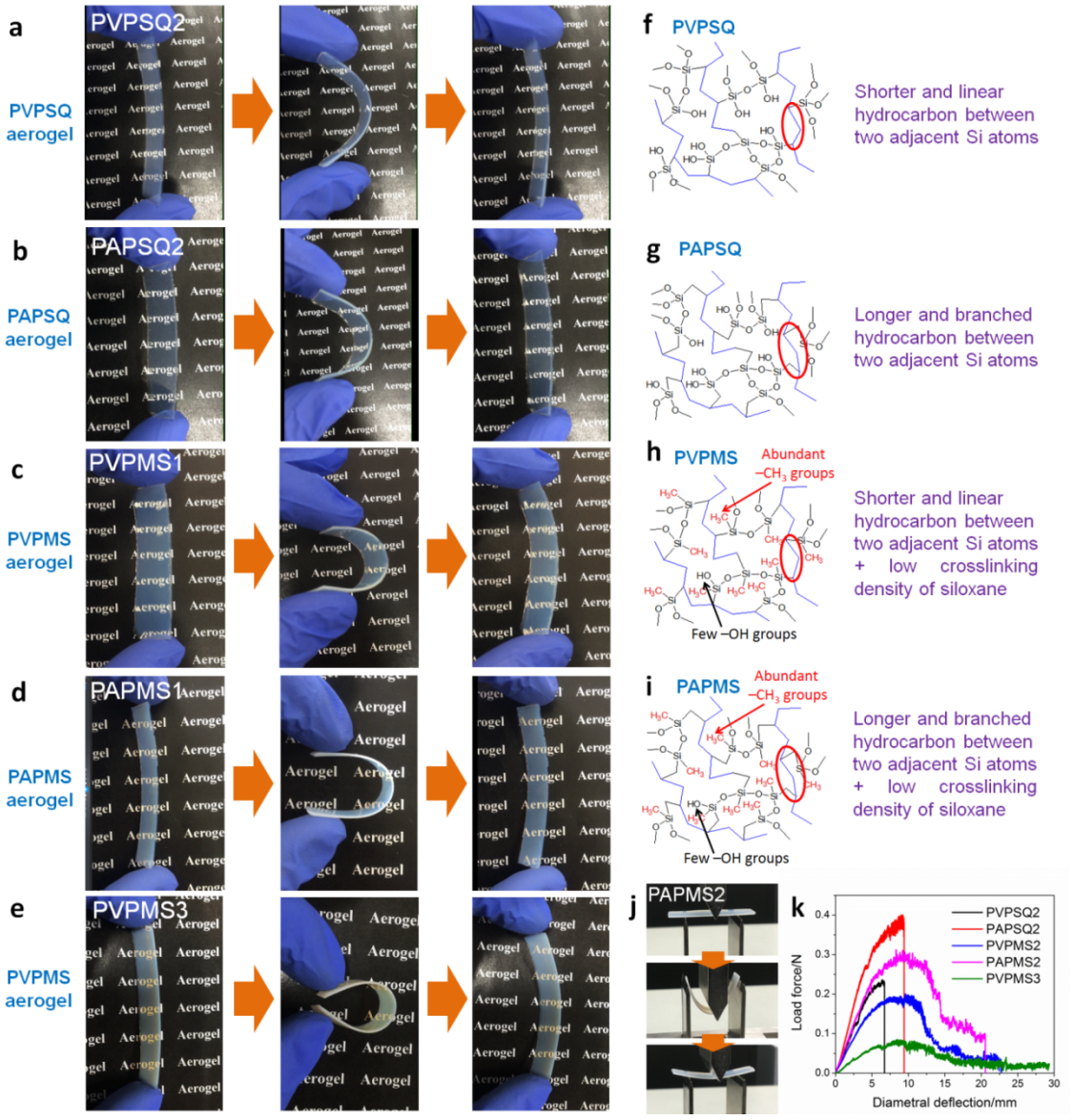

Figure 5. Bending flexibility of typical aerogels. (a-e) Hand bending tests on (a) PVPSQ2, (b) PAPSQ2, (c) PVPMS1, (d) PAPMS1, and (e) PVPMS3 aerogels. (f-i) Schematic of comparison

of different molecular-scaled structures of (f) PVPSQ, (g) PAPSQ, (h) PVPMS, and (i) PAPMS aerogels. (j) Photographs of a three-point bending test on PAPMS2. The fixture span is 25 mm and the thickness, width, and length of the aerogel are 1 mm, 10 mm, and 50-60 mm, respectively. (k) Stress-strain curves of three-point bending tests on typical PVPSQ, PAPSQ, PVPMS, and PAPMS aerogels.

The flexibility of PVPSQ, PAPSQ, PVPMS, and PAPMS aerogels and xerogels is significantly higher than that of traditional silica[9] and metal oxide aerogels.[40] In particular, the superflexibility of PVPMS and PAPMS aerogels/xerogels has not been observed in recently reported aerogels such as PMSQ,[15] PVSQ,[16] organo-bridged polysiloxanes,[18-20] nanocellulose,[22,23] chitosan,[24] polymer[3,27] and silica-based organic-inorganic hybrid aerogels.[11,13] In addition, the PVPMS aerogels exhibit the similar bending flexibility but much higher elasticity against compression compared to those of a commercial phenol foam with a sufficiently low thermal conductivity of ~ 20 mW m^{-1} K^{-1} (Figure S10). As discussed later, it is noteworthy that the doubly cross-linked aerogels and xerogels with superior mechanical properties exhibit even lower thermal conductivities.

The high compression and bending flexibility of PVPSQ, PAPSQ, PVPMS, and PAPMS aerogels are mainly attributed to the combination of polysiloxanes and hydrocarbon chains that compose their structure. The higher elasticity of PAPSQ aerogels compared to that of PVPSQ aerogels is probably because the branched hydrocarbon part between two adjacent silicon atoms in the PAPSQ network (Figure 5g) contributes to enhanced (or faster) relaxation as compared to that of the linear hydrocarbon chain between two adjacent silicon atoms in the PVPSQ network (Figure 5f). In the case of PAPMS aerogels, the abundant methyl groups bonded to silicon

atoms lead to a lower cross-linking density with a smaller amount of –OH groups of the polysiloxanes (Figures 2c and 5i) compared with that of PVPSQ and PAPSQ aerogels. The lower cross-linking density renders higher deformability. The abundant methyl groups in the polymethylsiloxane network of PAPMS aerogels facilitate their recovery from compression and bending, while the smaller amount of –OH groups in the skeletons reduces the irreversible shrinkage during compression and bending. The compression and bending flexibility of PAPMS aerogels is therefore higher than that of PVPSQ and PAPSQ aerogels.

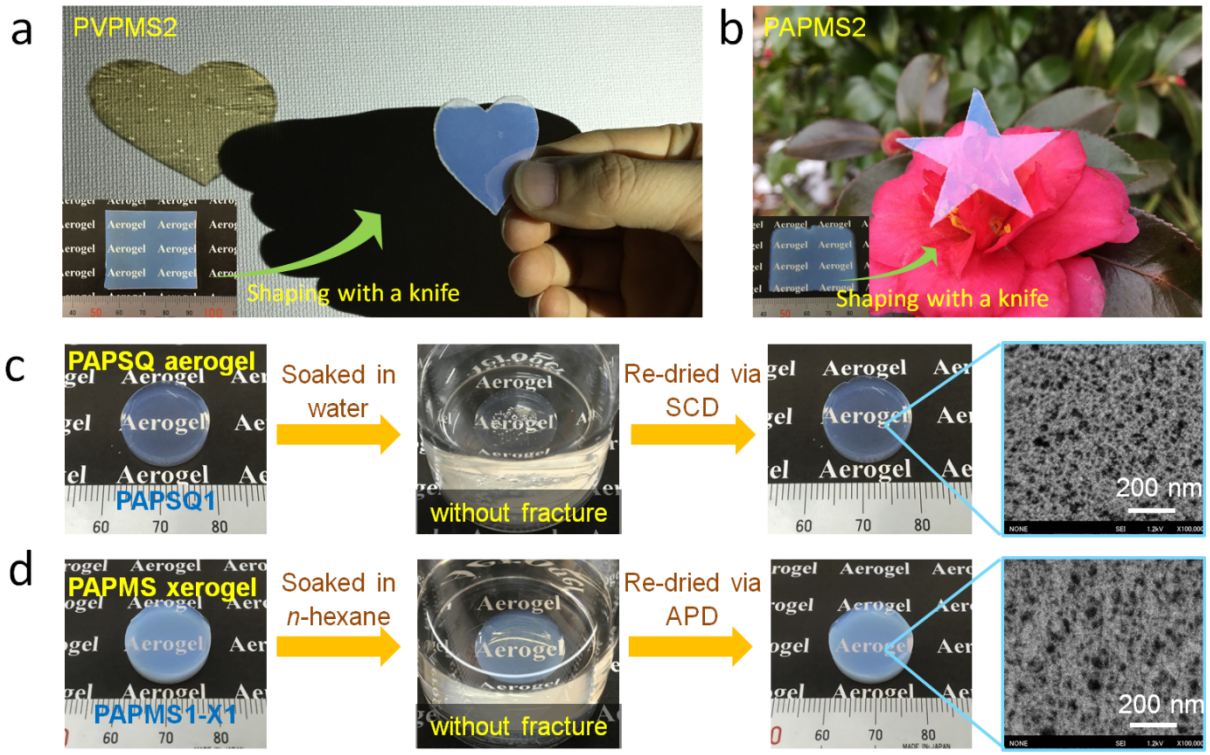

Figure 6. Excellent machinability of typical (a) PVPMS and (b) PAPMS aerogels shown by shaping with a knife. (c) The reprocessability of PAPSQ aerogel (PAPSQ1) shown by soaking in water and re-drying *via* SCD. (d) The reprocessability of PAPMS xerogel (PAPMS1-X1) shown by soaking in *n*-hexane and re-drying *via* APD.

In the case of PVPMS aerogels, they also show a doubly cross-linked structure with abundant methyl groups, a small amount of –OH groups and a low cross-linking density of polysiloxanes (Figure 5h), which leads to the similar flexibility as that of PAPMS aerogels. It it noteworthy that the bending flexibility of PVPMS3 (0.13 g cm^{-3}) is higher than that of PVPMS2 (0.19 g cm^{-3}) as shown in Figure 5c,e,k. This is probably attributed to the lower crosslinking density of polysiloxanes of aerogels with the lower bulk density.

In addition, transparent PVPSQ and PAPSQ aerogels can also be obtained *via* the same double-cross-linking method from vinyltriethoxysilane (VTES) and allyltriethoxysilane (ATES), respectively, which does not form toxic methanol in the course of the reactions (Figure S11). The PVPSQ and PAPSQ aerogels from VTES and ATES, respectively, exhibit the similar flexibility as that obtained from VTMS and ATMS.

The PAPSQ and PAPMS aerogels or xerogels also exhibit excellent reprocessability due to their toughness. The PAPSQ aerogel PAPSQ1 dried *via* SCD can be immersed in water without fracture and re-dried *via* SCD after solvent-exchange with IPA with its monolithicity, transparency and microstructure nearly unchanged (Figure 6c). In addition, the PAPMS xerogel PAPMS1-X1 dried *via* APD can be immersed in *n*-hexane without fracture and re-dried *via* APD with its transparency and microstructure nearly unchanged (Figure 6d). This indicates that these high-surface-area aerogels/xerogels can be used in a liquid phase or under humidity, which makes them even more suitable as adsorbents and catalyst supports as well as thermal superinsulators.

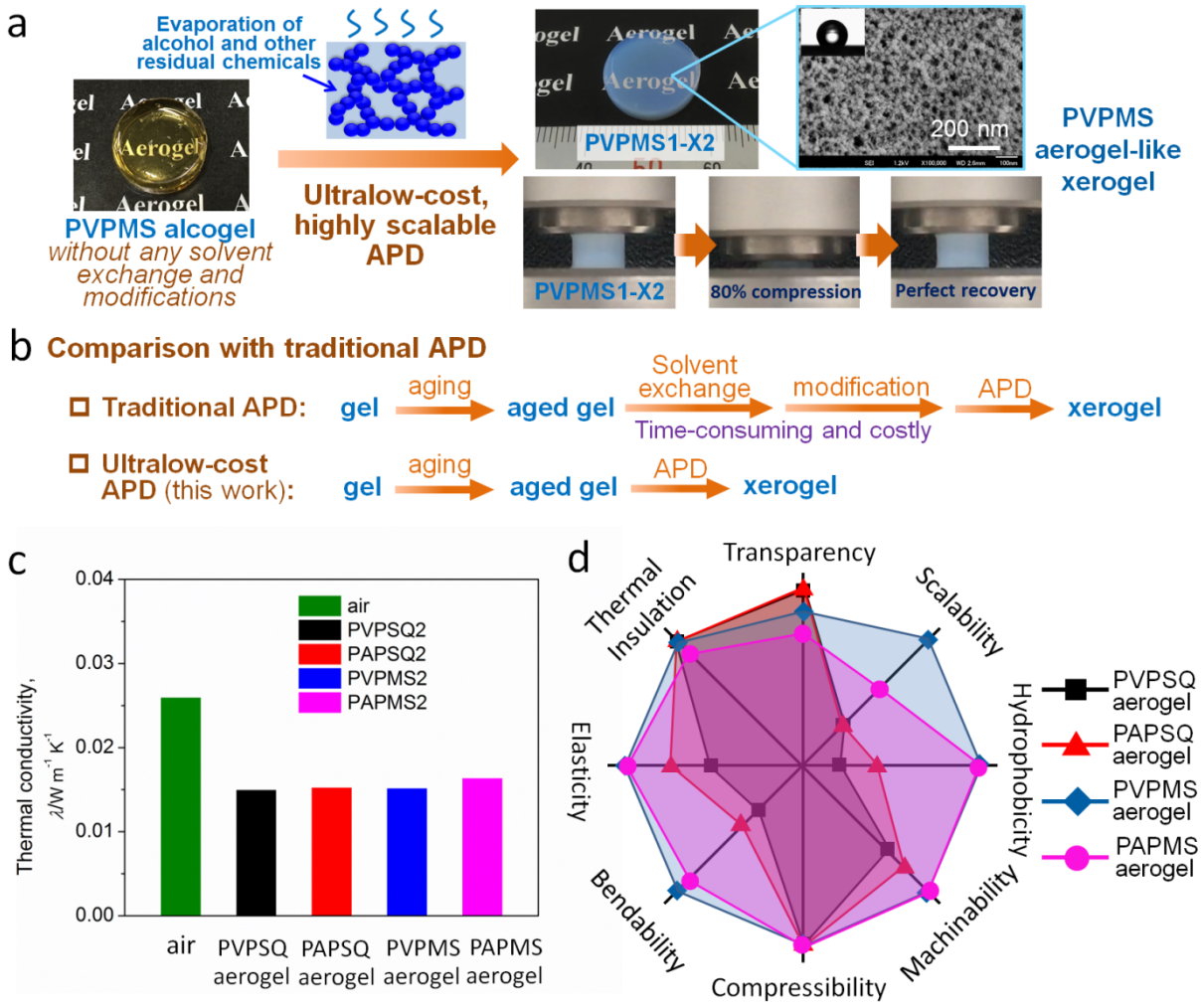

Figure 7. (a) Schematic of ultralow-cost APD without any solvent exchange and modifications and resultant transparent PVPMS aerogel-like xerogel PVPMS1-X2. The inset of the FESEM image presents the contact angle of water of 132°. (b) Comparison of our ultralow-cost APD and traditional APD. (c) Thermal conductivities of PVPSQ, PAPSQ, PVPMS, and PAPMS aerogels. (d) Qualitative comparison of typical properties of PVPSQ, PAPSQ, PVPMS, and PAPMS aerogels.

Due to its intrinsically hydrophobic and superflexible nature, transparent PVPMS aerogel-like xerogels (Table 1, Figure 7a) can be obtained by using IPA as the solvent in the

sol-gel process, followed by APD *without any solvent exchange and modifications*. The obtained PVPMS xerogels (PVPMS1-X2 and PVPMS2-X2) exhibit a homogeneous porous nanostructure with a low density of 0.19-0.23 g cm^{-3}, a high SSA of 716-770 m^2 g^{-1}, a narrow pore size distribution (Figure S12), and a high visible-light transmittance of 70-78% for 2 mm thick sample. They also show excellent mechanical properties with super-compressibility and superelasticity (Figure 7a, Movie S4). To the best of our knowledge, this is the first time to obtain transparent, low density, monolithic aerogel-like xerogels *via* APD without any solvent exchange and modifications. Since solvent exchange and modification that consume processing time and costs for solvent and modifiers are totally avoided (Figure 7b), their production cost can be further reduced, which will significantly contribute to their practical applications.

In addition to the excellent mechanical properties, the PVPSQ, PAPSQ, PVPMS, and PAPMS aerogels also exhibit outstanding thermal insulation properties. The total thermal conductivity (λ_{total}) of porous materials is mainly composed of solid (λ_s) and gas (λ_g) conductivities and radiation (λ_r): [41]

$$\lambda_{total} = \lambda_s + \lambda_g + \lambda_r \quad (1)$$

At room temperature, the total thermal conductivity is mainly determined by solid and gas conductivities due to the small contribution of radiation. On one side, the low bulk density (0.13-0.26 g cm^{-3}) and the interconnected nanoparticles network structure of these aerogels lead to low solid thermal conductivity. On the other side, the small pore size (mainly 10-70 nm) of these aerogels results in low gas thermal conductivity. As a result, the total thermal conductivities of PVPSQ2, PAPSQ2, PVPMS2, and PAPMS2 are as low as 15.0, 15.3, 15.2, and 16.4 mW m^{-1} K^{-1}, respectively, at room temperature and ambient pressure, showing a superinsulating performance (Table 1 and Figure 7c). These thermal conductivity values of the

aerogels in our work are comparable to those of conventional transparent silica (14-25 mW m^{-1} K^{-1}), [2,9] PVSQ (15.3 mW m^{-1} K^{-1})[16] and PMSQ (15-35 mW m^{-1} K^{-1})[14,42] aerogels and lower than those of transparent nanocellulose (18-38 mW m^{-1} K^{-1})[22,23] and chitosan (22-30 mW m^{-1} K^{-1})[24] aerogels and commercial thermal insulation materials such as polyurethane foam (PUF) (20-50 mW m^{-1} K^{-1}), phenol foam (20-50 mW m^{-1} K^{-1}), and mineral wool (35-80 mW m^{-1} K^{-1}). [10] A qualitative comparison of typical properties of PVPSQ, PAPSQ, PVPMS, and PAPMS aerogels is additionally provided in Figure 7d. The combination of low production cost, good transparency, high SSA, high hydrophobicity, excellent machinability, superflexibility in compression and bending, and superinsulating properties of PVPMS and PAPMS aerogels has not been observed in traditional aerogels.

CONCLUSION

A facile yet versatile double-cross-linking approach to transparent, highly flexible, machinable, superinsulating aerogels and xerogels is reported. A single alkenylalkoxysilane is first radically polymerized to obtain chain-like polyalkenylalkoxysilanes with high conversion, which are then subjected to hydrolytic polycondensation to afford a doubly cross-linked nanostructure consisting of polysiloxanes and hydrocarbon chains. Novel PVPSQ, PAPSQ, PVPMS, and PAPMS aerogels that are facilely prepared *via* this approach from VTMS (or VTES), ATMS (or ATES), VMDMS, and AMDMS, respectively, have been demonstrated. These aerogels exhibit an excellent combination of low density, uniform nanopores, high SSA, high transparency, high compression and bending flexibility, excellent machinability, and thermal superinsulation (λ=14.5-16.4 mW m^{-1} K^{-1}). In particular, because of the unique doubly cross-linked nanostructure with polymethylsiloxanes, transparent and superflexible PVPMS and PAPMS

aerogel-like xerogel superinsulators have been obtained *via* highly scalable APD without any solvent exchange and modifications for the first time, which significantly facilitates their production. These superior properties combined with the facile approach allow these aerogels and xerogels to be promising in the practical applications of transparent thermal superinsulators, catalyst support, sensors, etc.

ACKNOWLEDGEMENTS

Prof. Yasuyuki Nakamura, Prof. Shigeru Yamago, and Dr. Takehiro Fujita are acknowledged for their help in GPC. The NMR measurements were carried out in the JURC at the Institute for Chemical Research, Kyoto University. This study has been performed under financial supports from JSPS KAKENHI (Grant Numbers JP26288106 and 17K06015) and Advanced Low Carbon Technology Research and Development Program (ALCA, JST Japan).

ASSOCIATED CONTENT

Supporting Information

Results on the radical polymerization of different precursors, the effect of DTBP concentrations, multiple peak fitting on the solid-state NMR results, contact of typical aerogels/xerogels with water, FESEM images, N_2 adsorption/desorption measurements, photographs of mechanical tests on typical aerogels and xerogels, machinability, comparison with a commercial thermal insulation materials, compression and bending movies of typical aerogels and xerogels. This material is available free of charge *via* the Internet at http://pubs.acs.org.

REFERENCES

1. Prakash, S. S.; Brinker, C. J.; Hurd, A. J.; Rao, S. M. Silica Aerogel Films Prepared at Ambient Pressure by Using Surface Derivatization to Induce Reversible Drying Shrinkage. *Nature* **1995**, *374*, 439-443.
2. Huber, L.; Zhao, S.; Malfait, W. J.; Vares, S.; Koebel, M. M. Fast and Minimal-Solvent Production of Superinsulating Silica Aerogel Granulate. *Angew. Chem., Int. Ed.* **2017**, *56*, 4753-4756.
3. Ma, C. -B.; Du, B.; Wang, E. Self-Crosslink Method for a Straightforward Synthesis of Poly(Vinyl Alcohol)-Based Aerogel Assisted by Carbon Nanotube. *Adv. Funct. Mater.* **2017**, *27*, 1604423-1604431.
4. Si, Y.; Fu, Q.; Wang, X.; Zhu, J.; Yu, J.; Sun, G.; Ding, B. Superelastic and Superhydrophobic Nanofiber-Assembled Cellular Aerogels for Effective Separation of Oil/Water Emulsions. *ACS Nano* **2015**, *9*, 3791-3799.
5. Hees, T.; Zhong, F.; Rudolph, T.; Walther, A.; Mulhaupt, R. Nanocellulose Aerogels for Supporting Iron Catalysts and *in situ* Formation of Polyethylene Nanocomposites. *Adv. Funct. Mater.* **2017**, *27*, 1605586-1605593.
6. Lin, Z.; Zeng, Z.; Gui, X.; Tang, Z.; Zou, M.; Cao, A. Carbon Nanotube Sponges, Aerogels, and Hierarchical Composites: Synthesis, Properties, and Energy Applications. *Adv. Energy Mater.* **2016**, *6*, 1600554-1600579.
7. Cui, J.; Xi, Y.; Chen, S.; Li, D.; She, X.; Sun, J.; Han, W.; Yang, D.; Guo, S. Prolifera-Green-Tide as Sustainable Source for Carbonaceous Aerogels with Hierarchical Pore to Achieve Multiple Energy Storage. *Adv. Funct. Mater.* **2016**, *26,* 8487-8495.
8. Li, D.; Yang, D.; Yang, X.; Wang, Y.; Guo, Z.; Xia, Y.; Sun, S.; Guo, S. Double-Helix

Structure in Carrageenan–Metal Hydrogels: a General Approach to Porous Metal Sulfides/Carbon Aerogels with Excellent Sodium-Ion Storage. *Angew. Chem., Int. Ed.* **2016**, *55*, 15925-15928.

9. Wong, J. C. H.; Kaymak, H.; Brunner, S.; Koebel, M. M. Mechanical Properties of Monolithic Silica Aerogels Made from Polyethoxydisiloxanes. *Micropor. Mesopor. Mater.* **2014**, *183*, 23-29.
10. Pierre, A. C.; Pajonk, G. M. Chemistry of Aerogels and Their Applications. *Chem. Rev.* **2002**, *102,* 4243-4265.
11. Jiang, L.; Kato, K.; Mayumi, K.; Yokoyama, H.; Ito, K. One-Pot Synthesis and Characterization of Polyrotaxane−Silica Hybrid Aerogel. *ACS Macro Lett.* **2017**, *6*, 281-286.
12. Liu, A.; Medina, L.; Berglund, L. A. High-Strength Nanocomposite Aerogels of Ternary Composition: Poly(Vinyl Alcohol), Clay, and Cellulose Nanofibrils. *ACS Appl. Mater. Interfaces* **2017**, *9*, 6453-6461.
13. Zhao, S.; Zhang, Z.; Sebe, G.; Wu, R.; Virtudazo, R. V. R.; Tingaut, P.; Koebel, M. M. Multiscale Assembly of Superinsulating Silica Aerogels within Silylated Nanocellulosic Scaffolds: Improved Mechanical Properties Promoted by Nanoscale Chemical Compatibilization. *Adv. Funct. Mater.* **2015**, *25*, 2326-2334.
14. Hayase, G.; Kugimiya, K.; Ogawa, M.; Kodera, Y.; Kanamori, K.; Nakanishi, K. The Thermal Conductivity of Polymethylsilsesquioxane Aerogels and Xerogels with Varied Pore Sizes for Practical Application as Thermal Superinsulators. *J. Mater. Chem. A* **2014**, *2*, 6525-6531.
15. Kanamori, K.; Aizawa, M.; Nakanishi, K.; Hanada, T. New Transparent

Methylsilsesquioxane Aerogels and Xerogels with Improved Mechanical Properties. *Adv. Mater.* **2007**, *19*, 1589-1593.

16. Shimizu, T.; Kanamori, K.; Maeno, A.; Kaji, H.; Doherty, C. M.; Falcaro, P.; Nakanishi, K. Transparent, Highly Insulating Polyethyl- and Polyvinylsilsesquioxane Aerogels: Mechanical Improvements by Vulcanization for Ambient Pressure Drying. *Chem. Mater.* **2016**, *28*, 6860-6868.
17. Zou, F.; Yue, P.; Zheng, X.; Tang, D.; Fu, W.; Li Z. Robust and Superhydrophobic Thiourethane Bridged Polysilsesquioxane Aerogels as Potential Thermal Insulation Materials. *J. Mater. Chem. A* **2016**, *4*, 10801-10805.
18. Wang, Z.; Dai, Z.; Wu, J.; Zhao, N.; Xu, J. Vacuum-Dried Robust Bridged Silsesquioxane Aerogels. *Adv. Mater.* **2013**, *25*, 4494-4497.
19. Shimizu, T.; Kanamori, K.; Maeno, A.; Kaji, H.; Nakanishi, K. Transparent Ethylene-Bridged Polymethylsiloxane Aerogels and Xerogels with Improved Bending Flexibility. *Langmuir* **2016**, *32*, 13427-13434.
20. Shimizu, T.; Kanamori, K.; Maeno, A.; Kaji, H.; Doherty, C. M.; Nakanishi, K. Transparent Ethenylene-Bridged Polymethylsiloxane Aerogels: Mechanical Flexibility and Strength and Availability for Addition Reaction. *Langmuir* **2017**, *33*, 4543-4550.
21. Aoki, Y.; Shimizu, T.; Kanamori, K.; Maeno, A.; Kaji, H.; Nakanishi, K. Low-Density, Transparent Aerogels and Xerogels Based on Hexylene-Bridged Polysilsesquioxane with Bendability. *J. Sol-Gel. Sci. Technol.* **2017**, *81*, 42-51.
22. Kobayashi, Y.; Saito, T.; Isogai, A. Aerogels with 3D Ordered Nanofiber Skeletons of Liquid-Crystalline Nanocellulose Derivatives as Tough and Transparent Insulators. *Angew. Chem., Int. Ed.* **2014**, *53*, 10394-10397.

23. Mi, Q.; Ma, S.; Yu, J.; He, J.; Zhang, J. Flexible and Transparent Cellulose Aerogels with Uniform Nanoporous Structure by a Controlled Regeneration Process. *ACS Sustainable Chem. Eng.* **2016**, *4*, 656-660.

24. Takeshita, S.; Yoda, S. Chitosan Aerogels: Transparent, Flexible Thermal Insulators. *Chem. Mater.* **2015**, *27*, 7569-7572.

25. Wang, J. ; Zhang, X. Binary Crystallized Supramolecular Aerogels Derived from Hostguest Inclusion Complexes. *ACS Nano* **2015**, *9*, 11389-11397.

26. Khan, Z. U.; Edberg, J.; Hamedi, M. M.; Gabrielsson, R.; Granberg, H.; Wagberg, L.; Engquist, I.; Berggren, M.; Crispin, X. Thermoelectric Polymers and Their Elastic Aerogels. *Adv. Mater.* **2016**, *28*, 4556-4562.

27. Hasegawa, G.; Shimizu, T.; Kanamori, K.; Maeno, A.; Kaji, H.; Nakanishi, K. Highly Flexible Hybrid Polymer Aerogels and Xerogels Based on Resorcinol-Formaldehyde with Enhanced Elastic Stiffness and Recoverability: Insights into the Origin of Their Mechanical Properties. *Chem. Mater.* **2017**, *29*, 2122-2134.

28. Gong, J. P.; Katsuyama, Y.; Kurokawa, T.; Osada, Y. Double-Network Hydrogels with Extremely High Mechanical Strength. *Adv. Mater.* **2003**, *15*, 1155-1158.

29. Nonoyama, T.; Wada, S.; Kiyama, R.; Kitamura, N.; Mredha, M. T. I.; Zhang, X.; Kurokawa, T.; Nakajima, T.; Takagi, Y.; Yasuda, K.; Gong, J. P. Double-Network Hydrogels Strongly Bondable to Bones by Spontaneous Osteogenesis Penetration. *Adv. Mater.* **2016,** *28*, 6740-6745.

30. Zhang, H. J.; Sun, T. L.; Zhang, A. K.; Ikura, Y.; Nakajima, T.; Nonoyama, T.; Kurokawa, T.; Ito, O.; Ishitobi, H.; Gong, J. P. Tough Physical Double-Network Hydrogels Based on Amphiphilic Triblock Copolymers. *Adv. Mater.* **2016**, *28*, 4884-4890.

31. Gunji, T.; Kawaguchi, Y.; Okonogi, H.; Sakan, T.; Arimitsu, K.; Abe, Y. Preparation and Properties of Organic-Inorganic Hybrid Gel Films Based on Polyvinylpolysilsesquioxane Synthesized from Trimethoxy(vinyl)silane. *J. Sol-Gel Sci. Technol.* **2005**, *33*, 9-13.

32. Abe, Y.; Namiki, T.; Tuchida, K.; Nagao, Y.; Misono, T. Preparation and Properties of Silicon-Containing Hybrid Gels from Vinyltrimethoxysilane. *J. Non-Cryst. Solids* **1992,** *147&148*, 47-51.

33. Zu, G.; Shimizu, T.; Kanamori, K.; Zhu, Y.; Maeno, A.; Kaji, H.; Shen, J.; Nakanishi, K. Transparent, Superflexible Doubly Cross-linked Polyvinylpolymethylsiloxane Aerogel Superinsulators *via* Ambient Pressure Drying. *ACS Nano* DOI: 10.1021/acsnano.7b07117.

34. Loy, D. A.; Baugher, B. M.; Baugher, C. R.; Schneider, D. A.; Rahimian, K. Substituent Effects on the Sol-Gel Chemistry of Organotrialkoxysilanes. *Chem. Mater.* **2000**, *12*, 3624-3632.

35. Shimada, T.; Aoki, K.; Shinoda, Y.; Nakamura, T.; Tokunaga, N.; Inagaki, S.; Hayashi, T. A New Method of Covalent Attachment of Organic Functional Groups on Silica Gel. *J. Am. Chem. Soc.* **2003**, *125*, 4688-4689.

36. Park, J. -W.; Jun, C. -H. Transition-Metal-Catalyzed Immobilization of Organic Functional Groups onto Solid Supports through Vinylsilane Coupling Reactions. *J. Am. Chem. Soc.* **2010**, *132*, 7268-7269.

37. Hayase, G.; Kanamori, K.; Fukuchi, M.; Kaji, H.; Nakanishi, K. Facile Synthesis of Marshmallow-like Macroporous Gels Usable under Harsh Conditions for the Separation of Oil and Water. *Angew. Chem., Int. Ed.* **2013**, *52*, 1986-1989.

38. Hong, J. Y.; Bak, B. M.; Wie, J. J.; Kong, J.; Park, H. S. Reversibly Compressible, Highly Elastic, and Durable Graphene Aerogels for Energy Storage Devices under Limiting

Conditions. *Adv. Funct. Mater.* **2015**, *25*, 1053-1062.

39. Moitra, N.; Ichii, S.; Kamei, T.; Kanamori, K.; Zhu, Y.; Takeda, K.; Nakanishi, K.; Shimada, T. Surface Functionalization of Silica by Si−H Activation of Hydrosilanes. *J. Am. Chem. Soc.* **2014**, *136*, 11570-11573.
40. Zu, G.; Shen, J.; Wang, W.; Zou, L.; Lian, Y.; Zhang, Z.; Liu, B.; Zhang, F. Robust, Highly Thermally Stable, Core−Shell Nanostructured Metal Oxide Aerogels as High-Temperature Thermal Superinsulators, Adsorbents, and Catalysts. *Chem. Mater.* **2014**, *26*, 5761-5772.
41. Lu, X.; Arduini-schuster, M. C.; Kuhn, J.; Nilsson, O.; Fricke, J.; Pekala, R. W. Thermal Conductivity of Monolithic Organic Aerogels. *Science* **1992**, *255*, 971-972.
42. Hayase, G.; Kanamori, K.; Abe, K.; Yano, H.; Maeno, A.; Kaji, H.; Nakanishi, K. Polymethylsilsesquioxane−Cellulose Nanofiber Biocomposite Aerogels with High Thermal Insulation, Bendability, and Superhydrophobicity. *ACS Appl. Mater. Interfaces* **2014**, *6*, 9466-9471.

This is the original manuscript before revision.

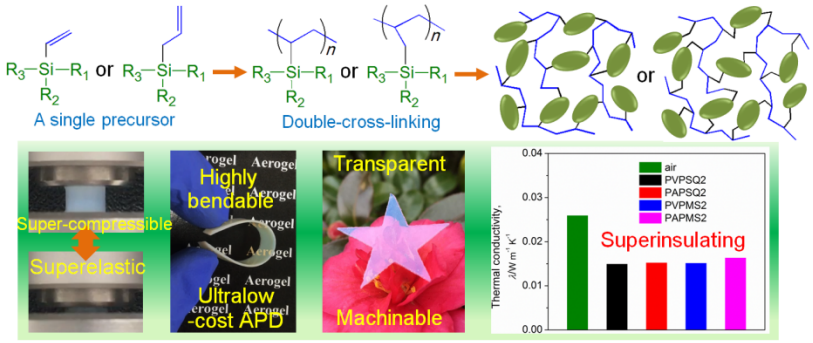

For Table of Contents Only